

# Investigations on the Synthesis and Properties of $\text{Fe}_2\text{O}_3/\text{Bi}_2\text{O}_2\text{CO}_3$ in the Photocatalytic and Fenton-like Process

Dongxue Sun<sup>1</sup>, Tingting Shen<sup>1</sup>, Jing Sun<sup>1</sup>, Chen Wang<sup>1</sup> and Xikui Wang<sup>2\*</sup>

<sup>1</sup>College of Environmental Science and Engineering, Qilu University of Technology, Jinan, Shandong, 250353, P.R. China,

<sup>2</sup>College of Environmental Science and Engineering, Shandong Agriculture and Engineering University, Jinan, Shandong, 251100, P.R. China.

\*xk\_wang@qlu.edu.cn

**Abstract.** Catalyst of  $\text{Bi}_2\text{O}_2\text{CO}_3$  and  $\text{Fe}_2\text{O}_3$  modified  $\text{Bi}_2\text{O}_2\text{CO}_3$  ( $\text{Fe}_2\text{O}_3/\text{Bi}_2\text{O}_2\text{CO}_3$ ) were prepared by hydrothermal method and characterized by X-ray diffractions (XRD), scanning electron microscopy (SEM), transmission electron microscope (TEM) and UV-vis DRS. The catalytic activity of  $\text{Bi}_2\text{O}_2\text{CO}_3$  and  $\text{Fe}_2\text{O}_3/\text{Bi}_2\text{O}_2\text{CO}_3$  were comparatively investigated in the photodegradation and Fenton-like process. Rhodamine B(RhB) was selected as the target pollutant under the irradiation of 300 W xenon lamp. The results indicated that  $\text{Fe}_2\text{O}_3$  plays a great role in the enhancing the treatment efficiency and the maximum reaction rate was achieved at the  $\text{Fe}_2\text{O}_3$  loading of 1.5%. The Fenton-like degradation rate constant of RhB with bare  $\text{Bi}_2\text{O}_2\text{CO}_3$  in dark is  $0.4 \text{ min}^{-1}$ , while that with 1.5  $\text{Fe}_2\text{O}_3/\text{Bi}_2\text{O}_2\text{CO}_3$  increases to  $28.4 \text{ min}^{-1}$  under visible light irradiation, a 71-fold improvement. It is expected to shed a new light for the constructing novel composite photocatalyst and also provide a potential method for the removal of dyes in the aqueous system.

## 1. Introduction

$\text{Bi}_2\text{O}_2\text{CO}_3$  is a typical Sillén-phase compound, in which the Bi-O atoms layer and  $\text{CO}_3^{2-}$  layer is orthogonal staggered symbiosis [1]. This structure can improve the separation efficiency of electron-hole pairs [2]. However, with a low absorption of UV light (about 5% of the solar light [3]), the application of  $\text{Bi}_2\text{O}_2\text{CO}_3$  photocatalytic materials is limited. Recently, many methods have been employed to overcome its limitations, including heterojunction fabrication. Tian et al. [4] compounded  $\text{Ag-C}_3\text{N}_4$  and  $\text{Bi}_2\text{O}_2\text{CO}_3$  and studied its photocatalytic performance. Wang et al. [3] successfully prepared the composite catalyst of  $\text{Bi}_2\text{O}_2\text{CO}_3/\text{g-C}_3\text{N}_4$  for the first time. This kind of catalyst exhibits high photocatalytic activity on NO in air degradation. Puttaswamy Madhusudan [5] compounded  $\text{BiVO}_4$  and  $\text{Bi}_2\text{O}_2\text{CO}_3$ , which can significantly improve its performance. Lin et al. [6] synthesized  $\text{Bi}_2\text{O}_2\text{CO}_3$  and  $\text{Bi}_2\text{MoO}_6$  via a one-pot hydrothermal method. Good photocatalytic activity can be attributed to the heterojunction interface which facilitates the separation of photogenerated electron-hole pairs. Zai et al. [7] researched I-doped  $\text{Bi}_2\text{O}_2\text{CO}_3$  and the catalyst exhibits high photocatalytic activity. Lv et al. [8] prepared  $\text{Bi}_2\text{O}_2\text{CO}_3/\text{TiO}_2$  composite powders which showed that the composite powders have a high photocatalytic activity than  $\text{TiO}_2$ . Furthermore,  $\text{Fe}_2\text{O}_3$  [9], a photocatalyst, has also been studied.

AOPs (advanced oxidation processes) has an efficient oxidization ability for organic pollutants, has become an important research task in the field of environmental protection [10], in which Fenton



reaction as a fast-growing AOPs technology[11]. Normal Fenton reaction uses the chain reaction between bivalent iron ion ( $\text{Fe}^{2+}$ ) and hydrogen peroxide ( $\text{H}_2\text{O}_2$ ) to generate strong oxidation ability and high electronegativity of hydroxyl radicals, most of the organic material in water can be oxidized. Its harsh conditions greatly limits the application in organic wastewater treatment( $\text{pH}<3$ ). Studies found that photo-Fenton system generated active ferric iron ligand which can regenerate ferrous iron ion through the transfer between ligand-metal charge under visible light. Therefore, finding visible light response catalyst which can efficiently use the solar energy light becomes a new direction in visible light photo-Fenton research.

In this paper, composite catalyst  $\text{Fe}_2\text{O}_3/\text{Bi}_2\text{O}_2\text{CO}_3$  was synthesized by a one-pot hydrothermal method. Especially, N, N-dimethylformamide (DMF) as a carbon source which was used for synthetic  $\text{Bi}_2\text{O}_2\text{CO}_3$  was used for the first time. The prepared samples were characterized and utilized as a kind of catalyst for the degradation of organic dye under Fenton synergistic effect. The research shows that it is an alternative technology for organic pollutants in wastewater treatment and has broad application prospects.

## 2. Experimental section

### 2.1. Preparation of $\text{Bi}_2\text{O}_2\text{CO}_3$ and $\text{Fe}_2\text{O}_3/\text{Bi}_2\text{O}_2\text{CO}_3$ photocatalysts

All the chemicals were used as received without any further purification. To obtain  $\text{Bi}_2\text{O}_2\text{CO}_3/\text{Fe}_2\text{O}_3$  samples,  $\text{Bi}(\text{NO}_3)_3 \cdot 5\text{H}_2\text{O}$  (2 mmol) was dissolved in 30 mL diluted  $\text{HNO}_3$  (2 M) and stirred for 30 minutes. Then  $\text{Fe}(\text{NO}_3)_3 \cdot 9\text{H}_2\text{O}$  was added into the above solution. The mixed solution was also stirred for another 4 hours. Thirdly, the pH was adjusted to 7.0 using ammonia solution under stirring. The fixed solution should be stirred for another 2 hours. With the increasing of the quantity of  $\text{Fe}(\text{NO}_3)_3 \cdot 9\text{H}_2\text{O}$ , the color of the final precursor was brown deepen. Fourthly, 5 mL DMF was added to above solution. Then the precursor was transferred into a 60 mL Teflon autoclave and maintained at  $200^\circ\text{C}$  for 10 hours. Subsequently, after cooling to room temperature, the products were washed with absolute ethanol and distilled water for several times, then freeze-drying. Especially, The preparation of pure  $\text{Bi}_2\text{O}_2\text{CO}_3$  is also described as above, except that it is not necessary to add  $\text{Fe}(\text{NO}_3)_3 \cdot 9\text{H}_2\text{O}$ . The final products were described according to the molar percent of  $\text{Fe}(\text{NO}_3)_3 \cdot 9\text{H}_2\text{O}$  used, the as-prepared catalysts were marked as  $\text{Bi}_2\text{O}_2\text{CO}_3$ , 0.1  $\text{Fe}_2\text{O}_3/\text{Bi}_2\text{O}_2\text{CO}_3$ , 0.5  $\text{Fe}_2\text{O}_3/\text{Bi}_2\text{O}_2\text{CO}_3$ , 1.0  $\text{Fe}_2\text{O}_3/\text{Bi}_2\text{O}_2\text{CO}_3$ , 1.5  $\text{Fe}_2\text{O}_3/\text{Bi}_2\text{O}_2\text{CO}_3$ , 2.0  $\text{Fe}_2\text{O}_3/\text{Bi}_2\text{O}_2\text{CO}_3$ .

### 2.2. Materials characterization

The catalyst was characterized via powder X-ray diffraction (XRD) with Cu K $\alpha$  radiation ( $\lambda = 1.5404 \text{ \AA}$ ) at a scan rate of  $0.05^\circ 2\theta/\text{s}$ . The morphology of the samples were examined by scanning electron microscope (SEM: Hitachi, Japan) and transmission electron microscope (TEM: JEOL, Japan). UV-Vis spectra was achieved by UV-Vis DRS spectrophotometer (U-3900H, Hitachi, Japan) over a range of 100~800 nm using  $\text{BaSO}_4$  as a reference.

### 2.3. Photocatalytic activity measurements

The catalysts were evaluated by the degradation of RhB at room temperature. The visible light source was a 300 W Xenon lamp with a cutoff filter ( $\lambda < 420 \text{ nm}$ ). Before irradiation, the suspension was magnetically stirred in the dark for 30 min to achieve adsorption/desorption equilibrium. 0.075 g catalyst was mixed with 1 mmol/L of  $\text{H}_2\text{O}_2$ . 150 mL RhB solution (RhB of 50 mg/L, pH 3.0) was mixed with the above mixture of catalyst and hydrogen peroxide. 3 mL of solution was taken every five minutes to test. The degradation of RhB was monitored by UV-Vis spectrophotometer.

### 3. Results and discussion

#### 3.1. Crystal structure analysis

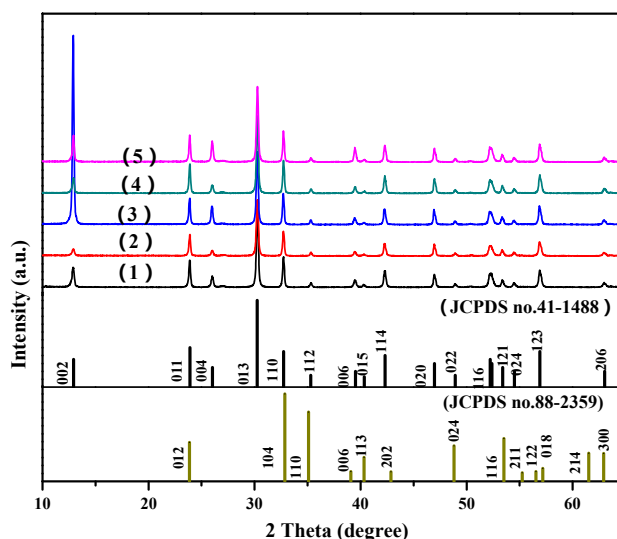


**Figure 1.** XRD patterns of  $\text{Bi}_2\text{O}_2\text{CO}_3$ (1),  $0.1 \text{ Fe}_2\text{O}_3/\text{Bi}_2\text{O}_2\text{CO}_3$ (2),  $1.0 \text{ Fe}_2\text{O}_3/\text{Bi}_2\text{O}_2\text{CO}_3$ (3),  $1.5 \text{ Fe}_2\text{O}_3/\text{Bi}_2\text{O}_2\text{CO}_3$ (4),  $2.0 \text{ Fe}_2\text{O}_3/\text{Bi}_2\text{O}_2\text{CO}_3$ (5) samples.

Figure 1 shows the composites of  $\text{Bi}_2\text{O}_2\text{CO}_3$  (JCPDS card no.41-1488) and  $\text{Fe}_2\text{O}_3$  (JCPDS card no.88-2359). It is clear that the prepared catalyst is tetragonal structure. No other diffraction peaks were observed, and the sharp and intense peaks indicate a good crystalline nature. The lattice fringes of the composite catalysts match well, which can be confirmed by the overlapped peaks between  $\text{Fe}_2\text{O}_3$  at  $23.85^\circ$  (012),  $32.86^\circ$  (104),  $35.08^\circ$  (110),  $39.08^\circ$  (006),  $40.32^\circ$  (113),  $42.87^\circ$  (202),  $48.83^\circ$  (024),  $53.51^\circ$  (116),  $55.25^\circ$  (211),  $56.54^\circ$  (122) and  $\text{Bi}_2\text{O}_2\text{CO}_3$  at  $23.90^\circ$  (011),  $32.73^\circ$  (110),  $35.31^\circ$  (112),  $39.51^\circ$  (006),  $40.36^\circ$  (015),  $42.30^\circ$  (114),  $48.93^\circ$  (022),  $53.41^\circ$  (121),  $54.51^\circ$  (024),  $56.90^\circ$  (123). This is good for the  $\text{Fe}_2\text{O}_3$  modification on the surface of  $\text{Bi}_2\text{O}_2\text{CO}_3$ . Furthermore, the lattice fringe of  $\text{Bi}_2\text{O}_2\text{CO}_3$  and  $\text{Fe}_2\text{O}_3$  matches so well that it could be ascribed to mixture of the characteristic peak of  $\text{Bi}_2\text{O}_2\text{CO}_3$  and  $\text{Fe}_2\text{O}_3$ . However, the new occurred impurity peak should be confirmed by the following characterization ways.

#### 3.2. Morphology characterization

It was found that  $\text{Bi}_2\text{O}_2\text{CO}_3$  (Figure 2a) and  $\text{Fe}_2\text{O}_3/\text{Bi}_2\text{O}_2\text{CO}_3$  (Figure 2b) showed the similar morphological structure as nano-chips, which could be accounted for the limited doping amount of  $\text{Fe}_2\text{O}_3$ . The SEM further indicated that the catalyst powder was uniformly dispersed without large-scale agglomeration. In addition, the results of TEM indicate that the catalyst has a length of about 250 nm and the thickness is about 20 nm. This is consistent with existing literature reports [12].

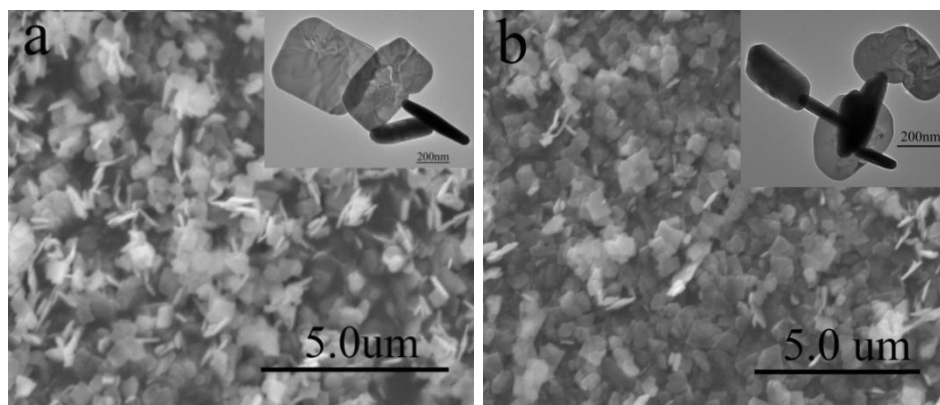


**Figure 2.** SEM and TEM (inserted graph) of pure  $\text{Bi}_2\text{O}_2\text{CO}_3$  (a) and  $1.5 \text{ Fe}_2\text{O}_3/\text{Bi}_2\text{O}_2\text{CO}_3$  (b).

### 3.3. UV-Vis-DRS analysis

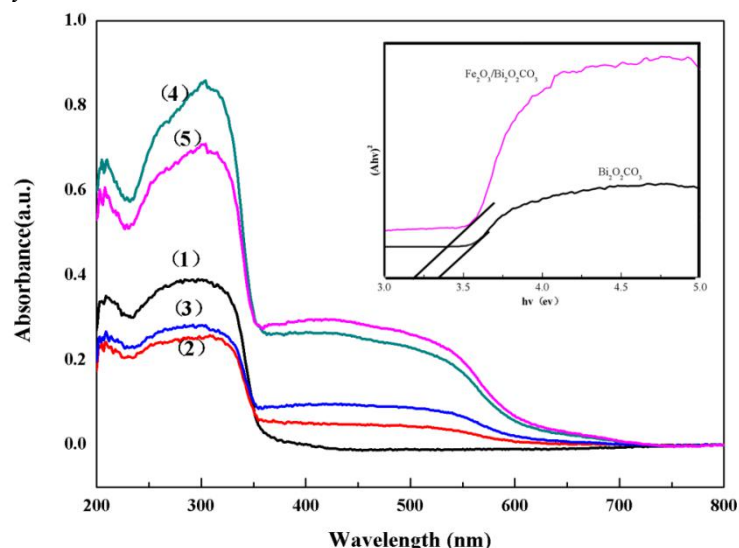


**Figure 3.** UV-Vis-DRS absorption spectra of  $\text{Bi}_2\text{O}_2\text{CO}_3$  (1),  $0.1 \text{ Fe}_2\text{O}_3/\text{Bi}_2\text{O}_2\text{CO}_3$  (2),  $1.0 \text{ Fe}_2\text{O}_3/\text{Bi}_2\text{O}_2\text{CO}_3$  (3),  $1.5 \text{ Fe}_2\text{O}_3/\text{Bi}_2\text{O}_2\text{CO}_3$  (4),  $2.0 \text{ Fe}_2\text{O}_3/\text{Bi}_2\text{O}_2\text{CO}_3$  (5) and the forbidden band width of  $\text{Bi}_2\text{O}_2\text{CO}_3$  and  $\text{Fe}_2\text{O}_3/\text{Bi}_2\text{O}_2\text{CO}_3$ .

It is very important to study the UV-vis absorption spectra as the semiconductor band structure is an important factor in determining the photocatalytic activity. Figure 3 shows the absorption spectra of different ratios of  $\text{Fe}_2\text{O}_3$  in the composite catalyst. As can be seen from the figure, the pure  $\text{Bi}_2\text{O}_2\text{CO}_3$  can only absorb UV light ( $\lambda$  is about 360 nm), and with the increase of  $\text{Fe}_2\text{O}_3$  deposition, the absorption peak of  $\text{Fe}_2\text{O}_3$  is seen at  $\lambda$  equals to 380 nm. The co-existence of  $\text{Fe}_2\text{O}_3$  and  $\text{Bi}_2\text{O}_2\text{CO}_3$  also indicates that the final composite catalyst has  $\text{Fe}_2\text{O}_3$ . In addition, the band width  $E_g$  follows the formula.

$$(\alpha h\nu)^{1/n} = C(h\nu - E_g) \quad (1)$$

Where  $\alpha$  is the absorption coefficient,  $h$  is the Planck constant,  $\nu$  is the frequency,  $C$  is constant. The index  $n$  is directly related to the type of semiconductor, direct band-gap semiconductor  $n=1/2$ , indirect band-gap semiconductor  $n=2$  [12]. It is known by the Lambert-Beer law that  $A$  is proportional to  $\alpha$ , and  $A$  is the absorbance in the visible diffuse reflection.  $h\nu$  (denoted by  $1240/\text{wavelength}$ ) is the x-coordinate. The tangent line of  $(\alpha h\nu)^{1/n}$  is the graph of the vertical coordinate, and the tangent

line of the curve is equal to  $E_g$ . Figure 3 shows that the forbidden band width of the composite catalyst after doping was less than that of the pure  $\text{Bi}_2\text{O}_2\text{CO}_3$ . The electrons are more easily excited to produce the luminous carrier [4].

### 3.4. Effect of $\text{Fe}_2\text{O}_3$ loading on the Fenton-like reactivity of $\text{Bi}_2\text{O}_2\text{CO}_3$

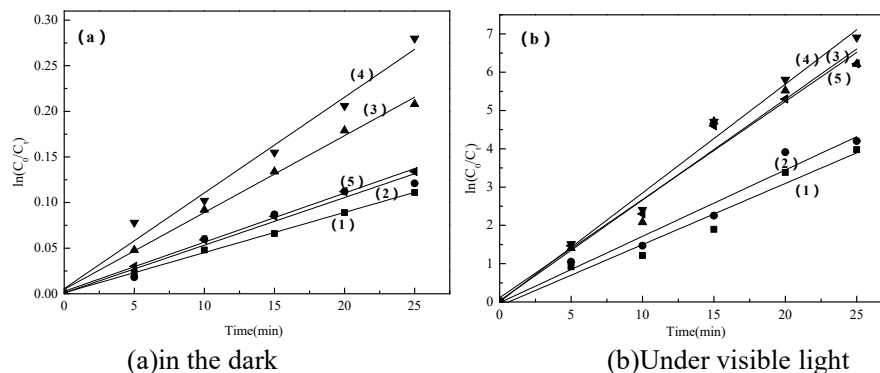


**Figure 4.** Fenton-like degradation of RhB with  $\text{Bi}_2\text{O}_2\text{CO}_3$  (1), 0.1  $\text{Fe}_2\text{O}_3/\text{Bi}_2\text{O}_2\text{CO}_3$  (2), 1.0  $\text{Fe}_2\text{O}_3/\text{Bi}_2\text{O}_2\text{CO}_3$  (3), 1.5  $\text{Fe}_2\text{O}_3/\text{Bi}_2\text{O}_2\text{CO}_3$  (4), 2.0  $\text{Fe}_2\text{O}_3/\text{Bi}_2\text{O}_2\text{CO}_3$  (5).

**Table 1.** Degradation rate constants of RhB of the  $\text{Bi}_2\text{O}_2\text{CO}_3$  and  $\text{Fe}_2\text{O}_3/\text{Bi}_2\text{O}_2\text{CO}_3$  catalysts.

Samples	$k/\text{min}^{-1}$	
	In the dark	Under visible light
$\text{Bi}_2\text{O}_2\text{CO}_3$	0.4	15.9
0.1 $\text{Fe}_2\text{O}_3/\text{Bi}_2\text{O}_2\text{CO}_3$	0.5	17.4
1.0 $\text{Fe}_2\text{O}_3/\text{Bi}_2\text{O}_2\text{CO}_3$	0.8	26.3
1.5 $\text{Fe}_2\text{O}_3/\text{Bi}_2\text{O}_2\text{CO}_3$	1.0	28.4
2.0 $\text{Fe}_2\text{O}_3/\text{Bi}_2\text{O}_2\text{CO}_3$	0.5	25.6

Figure 4 investigates the degradation effect of RhB with various  $\text{Fe}_2\text{O}_3/\text{Bi}_2\text{O}_2\text{CO}_3$  catalytic systems. The Fenton-like response in the dark condition was achieved in Figure 4a, and the photo-Fenton-like reactivity under visible light irradiation was concluded in Figure 4b. The corresponding degradation rate constants of RhB of the  $\text{Bi}_2\text{O}_2\text{CO}_3$  and  $\text{Bi}_2\text{O}_2\text{CO}_3\text{-Fe}_2\text{O}_3$  catalysts are listed in Table 1.

In Figure 4a, the Fenton-like response conforms to the first order dynamic equation. With the increase of  $\text{Fe}_2\text{O}_3$  loading, the catalytic performance of the catalyst gradually increased, the maximum removal efficiency occurred in the system of 1.5  $\text{Fe}_2\text{O}_3/\text{Bi}_2\text{O}_2\text{CO}_3$ . The reaction rate of 1.5  $\text{Fe}_2\text{O}_3/\text{Bi}_2\text{O}_2\text{CO}_3$  is 2.5 times than that of  $\text{Bi}_2\text{O}_2\text{CO}_3$ . This indicates that a small amount of  $\text{Fe}_2\text{O}_3$  doping is beneficial to the enhancement of Fenton-like effect. Due to the  $\text{Fe}^{3+}$  components in the complex  $\text{Fe}_2\text{O}_3/\text{Bi}_2\text{O}_2\text{CO}_3$ , the Fenton reaction is bound to occur with the addition of  $\text{H}_2\text{O}_2$  as a catalytic agent. The RhB is partially oxidized and degraded.

Figure 4b shows the degradation effect of RhB under photo-Fenton-like degradation of pure  $\text{Bi}_2\text{O}_2\text{CO}_3$  and  $\text{Fe}_2\text{O}_3/\text{Bi}_2\text{O}_2\text{CO}_3$ . It was found that pure  $\text{Bi}_2\text{O}_2\text{CO}_3$  shows a good photo-Fenton catalytic effect on RhB. Moreover, the addition of  $\text{Fe}_2\text{O}_3$  enhances the photo-Fenton catalytic effect of the catalyst. Among them, the catalytic effect of 1.5  $\text{Fe}_2\text{O}_3/\text{Bi}_2\text{O}_2\text{CO}_3$  achieved the highest treatment efficiency, and the catalytic effect is 1.8 times that of pure  $\text{Bi}_2\text{O}_2\text{CO}_3$ . Notably, the photo-Fenton-like degradation effect of composite catalyst 1.5  $\text{Fe}_2\text{O}_3/\text{Bi}_2\text{O}_2\text{CO}_3$  under visible light is 71 times than that of pure  $\text{Bi}_2\text{O}_2\text{CO}_3$  under Fenton-like system in the dark.

Because of the response capacity of  $\text{Bi}_2\text{O}_2\text{CO}_3$  to visible light, and its microstructure can increase the catalytic activity point, the synergistic effect of these advantages and Fenton reaction make photocatalytic activity and degradation ability growing rapidly. This may be due to the fact that the photoelectric electron generated by  $\text{Fe}_2\text{O}_3$  is more likely to be transferred from its guide band to the guide band of  $\text{Bi}_2\text{O}_2\text{CO}_3$  [12]. The electron in the guide band of  $\text{Bi}_2\text{O}_2\text{CO}_3$  can react with the

adsorption of  $O_2$  in the dye solution through a series of reactions to generate  $H_2O_2$ , the accumulation of holes in the  $Fe_2O_3$  price band can react with the  $OH^-$  in the dye solution, then it produces  $\cdot OH$  with strong oxidation which is highly oxidized, while  $H_2O_2$  can also quickly obtained an electron which also produces the strong oxidizing of  $\cdot OH$  [11].

#### 4. Conclusions

In this paper,  $Bi_2O_2CO_3$  and  $Fe_2O_3/Bi_2O_2CO_3$  composite photocatalyst were successfully prepared by hydrothermal method. The final composite catalysts have a tetragonal phase with a nano-chip structure. The length of the composite catalysts is about 250 nm and the width of the thickness is about 20 nm. The addition of  $Fe_2O_3$  can accelerates the degradation efficiency of RhB dramatically. The results further reveals that  $Fe_2O_3/Bi_2O_2CO_3$  acts as a photo and a Fenton-like catalyst as well. It is expected to shed a new idea for the constructing novel composite photocatalyst and also provide a potential method for the removal of dyes in the aqueous system.

#### Acknowledgements

This work was supported by National Natural Science Foundation of China (Grant no. 21507067).

#### References

- [1] Cong R, Sun J, Yang T, et al. ChemInform Abstract: Syntheses and Crystal Structures of Two New Bismuth Hydroxyl Borates Containing  $[Bi_2O_2]^{2+}$  Layers:  $Bi_2O_2[B_3O_5(OH)]$  and  $Bi_2O_2[BO_2(OH)]$ . [J]. Cheminform, 2011, 42(32):no-no.
- [2] Yu C, Yu J C, Fan C, et al. Synthesis and characterization of Pt/BiOI nanoplate catalyst with enhanced activity under visible light irradiation[J]. Materials Science & Engineering B, 2010, 166(3):213-219.
- [3] Chi C T, Lu I F, Chiu I C, et al. Flexible Transparent ZnO:Al/ZnO/CuAlOx :Ca Heterojunction Diodes on Polyethylene Terephthalate Substrates[J]. Journal of Electronic Materials, 2013, 42(6):1242-1245.
- [4] Tian N, Huang H, Guo Y, et al. Ag- $C_3N_4/Bi_2O_2CO_3$ , composite with high visible-light-driven photocatalytic activity for rhodamine B degradation[J]. Applied Surface Science, 2014, 322:249-254.
- [5] Yan Z, Fang D, Chen M, et al. Synthetic  $Bi_2O_2CO_3$ , nanostructures: Novel photocatalyst with controlled special surface exposed[J]. Journal of Molecular Catalysis A Chemical, 2010, 317 (1-2):34-40.
- [6] Lin X, Guo X, Shi W, et al. Hydrothermal Synthesis of Mesh-Like  $Bi_2O_2CO_3/Bi_2MoO_6$  Heterojunction with Enhanced Photocatalytic Activity[J]. Nanoscience & Nanotechnology Letters, 2015, 7(9):691-696.
- [7] Zai J, Cao F, Liang N, et al. Rose-like I-doped  $Bi_2O_2CO_3$ , microspheres with enhanced visible light response: DFT calculation, synthesis and photocatalytic performance[J]. Journal of Hazardous Materials, 2016, 321:464.
- [8] Lv X, Tang Z L, Zhai X L, et al. Preparation and photocatalytic activities of  $Bi_2O_2CO_3/TiO_2$  composite powders[J]. Gongneng Cailiao/journal of Functional Materials, 2013, 44(12):1812-1815.
- [9] Wei Z, Wei X, Wang S, et al. Preparation and visible-light photocatalytic activity of  $\alpha-Fe_2O_3/\gamma-Fe_2O_3$ , magnetic heterophase photocatalyst[J]. Materials Letters, 2014, 118:107-110.
- [10] Goi A, Trapido M. Hydrogen peroxide photolysis, Fenton reagent and photo-Fenton for the degradation of nitrophenols: a comparative study[J]. Chemosphere, 2002, 46(6):913-22.
- [11] Nogueira R F, Oliveira M C, Paterlini W C. Simple and fast spectrophotometric determination of  $H_2O_2$  in photo-Fenton reactions using metavanadate. [J]. Talanta, 2005, 66(1):86.
- [12] Hu D, Zhang K, Yang Q, et al. Super-high photocatalytic activity of  $Fe_2O_3$ , nanoparticles anchored on  $Bi_2O_2CO_3$ , nanosheets with exposed {001} active facets[J]. Applied Surface Science, 2014, 316(1):93-101.